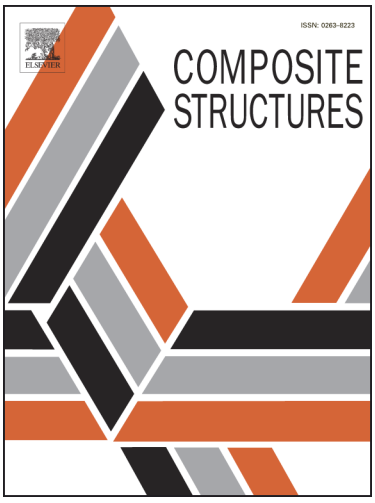

Parametric Study of Environmental Conditions on The Energy Harvesting Efficiency for The Multifunctional Composite Structures

Tao Wen, Alon Ratner, Yu Jia, Yu Shi

PII: S0263-8223(20)32905-6
DOI: https://doi.org/10.1016/j.compstruct.2020.112979
Reference: COST 112979

To appear in: *Composite Structures*

Received Date: 27 May 2020
Revised Date: 8 September 2020
Accepted Date: 11 September 2020

Please cite this article as: Wen, T., Ratner, A., Jia, Y., Shi, Y., Parametric Study of Environmental Conditions on The Energy Harvesting Efficiency for The Multifunctional Composite Structures, *Composite Structures* (2020), doi: https://doi.org/10.1016/j.compstruct.2020.112979

Parametric Study of Environmental Conditions on The Energy Harvesting Efficiency for The Multifunctional Composite Structures

Tao Wen[1], Alon Ratner[2], Yu Jia[3]*, Yu Shi[1]*

[1]Chester Smart Composites Group, University of Chester, Chester, UK

[2]Warwick Manufacturing Group, University of Warwick, Coventry, UK

[3]Mechanical Engineering and Design, Aston University, Birmingham, UK

*corresponding author: y.shi@chester.ac.uk; y.jia1@aston.ac.uk

Abstract

This paper presents a parametric study of the efficacy of an integrated vibration energy harvesting device under the environmental condition representative of an offshore wind turbine. A multifunctional glass fibre composite with an integrated Micro Fibre Composite (MFC) energy harvesting device was tested by swept sine vibration under environmental conditions that ranged from – 40°C to 70°C in temperature and 10%RH to 90%RH in humidity in order to characterise the sensitivity and dependence of energy harvesting on environmental conditions. Experimental vibration testing was complemented with theoretical analysis to investigate the relative contributions to the temperature dependence of energy harvesting. This included mechanical properties of the stiffness and strength of the cantilever structure and the electrical properties of the MFC transducer, including its dielectric constants and charge coefficients. An inverse proportionality was observed between the magnitude of harvested energy and the climatic temperature. The efficiency of energy harvesting was dominated by the stiffness of the cantilever, which displayed viscoelastic temperature dependence. The sample was also tested with a vibration profile obtained from a wind turbine in order to validate the temperature influence under typical service conditions. Numerical modal analysis was used to determine the shapes of resonance modes, the frequencies of which were temperature dependent. Humidity was observed to have a secondary influence on energy harvesting, with no significant short-term effect on the structural properties of the samples within the limits of the experimental method.

Keywords: Multifunctional composite structure, Energy harvesting, MFC.

Introduction

The increasingly widespread use of composites for lightweight structures has been encouraged by the continued development of new materials, including multifunctional composites [1, 2]. Multifunctional structures are valued for the efficiency with which they can provide additional functionalities that include Structural Health Monitoring (SHM) and energy harvesting, the latter of which has been demonstrated as a means of self-powering sensing and wireless communications [3, 4]. In contrast to wired sensors, considerable savings in the cost of manufacturing, time for assembly and weight reduction can be achieved by the use of remote sensors that do not rely on wired connections.

Moreover, the reliability of multifunctional sensors can be significantly greater as built-in functional elements that are co-manufactured into the composite benefit from the physical protection afforded by the encapsulating layer of resin that lasts beyond the lifetime of the product [5, 6]. There has been a growing interest in these multifunctional composites for a wide range of applications, from small consumer electronic devices and prosthetics to large vehicles, aerospace structures and civil infrastructure [7-12]. For instance, wireless sensor networks within multifunctional composites can provide SHM capabilities for wind turbine blades that are susceptible to damage and fatigue and thereby lower the maintenance cost of offshore wind energy [13-17]. Similarly, multifunctional composites can provide effective monitoring and communications for aerospace applications that require stringent optimisation of weight and reliability [18-20].

Low cost piezoelectric sensors have been shown to be suitable for harvesting vibrational energy in a wide range of applications [21, 22]. For example, Macro-Fibre Composite (MFC) devices that contain piezo ceramic rods and interdigitated electrodes have been reported to efficiently harvest energy when built into aerospace grade unidirectional composite structures [23, 24].

Piezoelectric based energy harvesting has been studied mostly with cantilever systems whereby the magnitude of harvested energy is proportional to the axial strain that arises due to the bending moment applied to the beam [25]. Energy is harvested optimally at the first mode of resonance of bending since this excitation results in the greatest axial strain in the cantilever. A benefit of this methodology is that this resonance can be directly measured from the voltage response of the piezoelectric device since it is maximal at the natural frequency of the structure [26, 27]. The efficacy of this approach for energy harvesting from an MFC embedded within a multifunctional composite has been reported in both experimental measurements and computational predictions by Shi et al. [28, 29]. Their research demonstrated energy harvesting from vibration profiles that replicated the service conditions of various industrial applications [28-30]. There is an outstanding need to explore the efficiency of energy harvesting in typical environmental conditions at different temperatures and humidity levels since aerospace and wind energy applications are typically required to operate in relatively harsh environmental conditions [31].

In this work, the temperature and humidity dependence of energy harvesting for multifunctional composites was studied with respect to factors that would affect the mechanical and electrical properties of composites and MFC energy harvesting devices [32, 33]. A series of vibration tests were conducted by replicating vibration profiles obtained from the in-service operation of wind turbines for a wide range of temperature and humidity levels that represented the environmental conditions experienced at an offshore wind farm. Parametric studies of the effect of temperature and humidity were undertaken to assess the efficacy of energy harvesting for realistic conditions of operation.

Fabrication of composite samples and experimental tests

The environmental parameters of temperature and humidity were experimentally measured for energy harvesting output by the multifunctional composite cantilever under vibration tests [30]. For this study, a woven fibre reinforced composite sample with an integrated MFC transducer was manufactured and tested; details of the fabrication process are provided in subsection section 2.1. The subsequent subsection section 2.2 explains how the sample was tested under certain environmental conditions and essential data processing used for excitation data.

2.1 Fabrication of multifunctional glass-fibre reinforced composites

12 plies of glass fibre reinforced VTC401 epoxy pre-preg (SHD Composite Material, UK) were cut into 60mm x 200mm strips and stacked ready for curing to obtain a cured laminate thickness of approximately 4mm. A Macro Fibre Composite (MFC) M8528-P2 (Smart Material, Germany) was selected for the energy harvester device; the active area of the sensor has dimensions of 85mm x 28mm x 0.3mm. To ensure maximum efficiency of energy harvesting with minimal losses, the MFC was laid up onto the top of the pre-preg plies and co-cured in a convection oven based on the curing conditions offered by the prepreg supplier. Release tape was used to protect the electrodes from the ingress of resin during the curing cycle and to ensure their readiness for connection with experimental facilities, as shown in Fig. 1.

2.2 Vibration tests set up

Dynamic vibration tests were undertaken with a Data Physics SignalForce GW-V617/DSA5-10K shaker with a Weiss VCV³ 4060-5 climatic test chamber at the Energy Innovation Centre in Warwick Manufacturing Group (WMG), University of Warwick. The sample was fastened to an aluminium 6082 fixture on the head expander of the shaker with a single M8 steel bolt tightened with a torque wrench to 10Nm. The fixture was instrumented with two PCB 256A32 piezoelectric accelerometers with cables that were rated for operation in the full range of temperatures attained by the climatic chamber. In order to avoid changing the resonance characteristics of the sample by adding mass to its structure, the accelerometers were placed onto the fixture as close as possible to the sample rather than onto the sample itself for the purpose of controlling and monitoring vibration tests. The MFC harvester was connected to a breadboard with a predefined 20kOhm load, which has been measured to be an optimal external load for the sample, as determined by previous work [29, 30]. The temperature was measured using K-type thermocouples placed at the edge of the sample and on the main body of the fixture. The temperature was recorded by a Pico TC-08 thermocouple data logger. The wires of the accelerometers and MFC sensor were connected to a Data Physics Abacus DSPcentric Signal Processing Hardware data acquisition system, which was used to control the drive voltage to the amplifier of the shaker and to monitor the signals from the sensors, as shown in Figs 2 and 3.

Energy harvesting was evaluated by swept sine tests in the frequency domain and by the replication of time-history collected from the offshore wind farm in the time domain. Swept sine tests were undertaken from 5Hz to 500Hz at a constant acceleration of 0.5g with a sweep rate of 2 octaves/minute and these were repeated three times for each environmental condition. The quoted acceleration in this work thus represents the mean value of each of the three tests. The electrical output of the MFC device was quantified as voltage RMS in the frequency domain. The mean voltage RMS from each swept sine was also calculated by averaging the voltage measured at each frequency interval.

A vibration profile for replication of random vibration from a wind turbine tower in an offshore wind farm was provided by Titan Wind Power. The sample was obtained in the form of a 60 seconds segment of acceleration in the time domain that was recorded at a rate of 8000Hz. This segment was resampled at a lower resolution of 5120Hz for compatibility with the sampling range of the shaker controller. Random tests were conducted by operating the shaker for a period of five minutes, which was achieved by consecutively repeating this 60 seconds segment 5 times. The mean voltage RMS was thus calculated for the whole 300 second period, for a total of 307200 data points for each random vibration test. Vibration testing was performed with the following procedure for each temperature and humidity set-point:

Adjust the temperature set-point and wait for hygrothermal equilibrium when the temperature of the thermocouple attached to the sample has stabilised to within ±0.5°C of the set-point temperature and the climatic chamber has stabilised at ±2%RH; this waiting period was necessary to allow the PID controller of the climatic chamber to adjust to the new set-point.

Repeat individual swept sine tests for 3 times.

Random vibration replication of wind turbine time-history for a period of 300 seconds.

The temperature effect on energy harvester

This section illustrates how the temperature dependence factors affect the energy harvester device based on theoretical analysis and experimental results. Firstly, a swept sine excitation test was undertaken to explore the overall trend of energy output with an increase in temperature. With reference to this trend, those factors that indirectly affect the energy output were theoretically deduced, analysed and compared with experimental results for verification. In the last subsection, an experiment to investigate the influence of temperature was carried out in an environment representing the humidity of a real offshore wind turbine in order to compare the results of the swept sine excitation test and to verify the reliability of the experimental results.

3.1 Swept sine tests and results analysis

Preliminary studies were undertaken to obtain the frequency range of the first several resonant modes of the sample, after which it was necessary to perform swept sine excitation to characterize the harvester device. In the experiment, the corresponding RMS voltage output value of each frequency was recorded instead of measuring the time domain when the frequency changes at a logarithmic rate, but essentially the same as in the time domain. The blue curve in Fig. 4 shows the change of RMS voltage generated by the integration system during the excitation frequency from 5Hz to 500Hz at a constant acceleration amplitude of 0.5g with a sweep rate of 2 octaves/minute (with a total duration of 3 minutes and 19 seconds). The measured temperature ranged from -40 to 70 °C, spaced at intervals of 10 °C. The humidity was set to 50%RH, as the wind blades are thought to be largely unaffected by structural defects related to humidity at a relative humidity below 50%RH [39]. From these subplots, it is simple to notice that their output voltage varies significantly at different test temperatures, especially the magnitude of the vertical axis. For ease of visualisation and reflecting the changing trend of these blue curves more intuitively, the trend lines were plotted through the data points using a Fourier fitting function, which is shown as red lines in Fig. 4. A common trend in all of the subgraphs is an increase in voltage from 5Hz to 100Hz, after which the curves tend towards a sinusoidal plateau. Variation in amplitude between tests conducted shows that temperature influenced the output voltage. But the position of the mutation cannot be reflected as the resonant frequency, as figure reflects the voltage amplitude generated by the system at various frequencies, rather than the frequency domain image converted from time frequency, therefore lack of accuracy. However, it could reflect a certain extent the temperature influence on energy output by calculating the average voltage of the sweep test. This establishes the assumption that temperature has an effect on the structure of the ensemble so that the research can proceed to the next step.

Figure 5 presents the averaged magnitudes of VRMS in the frequency domain for each measured temperature condition previously shown in Fig. 4, with a trend line smoothed through quadratic fitting shown in red. From the graph, it can be seen that the highest voltage was recorded at -10 °C, so this

is the optimal temperature for the integrated structure to generate energy. In addition, it shows a non-linear relationship between mean VRMS and temperature with a general trend of greater energy harvested at lower temperatures. Considering the composition of the sample, this trend suggests that the temperature dependence of the magnitude of the electrical output is affected by a multitude of factors, including the strain of mechanical deformation of the cantilever and the electrical properties of the MFC device. Meanwhile, the suitability of the MFC device for harvesting energy over a wide range of temperatures and its greater performance at lower temperatures indicates the relevance of this technology for the proposed examples of aerospace and wind energy applications since they are known to operate at extreme temperatures.

3.2 Theoretical analysis of related factors

MFC device considered by this investigation was contributed to by a variety of factors that influence the efficacy of energy harvesting. These include the dielectric constant and charge coefficient of electrical parameters of the MFC and the mechanical properties of the composite structure itself. The correlation between these parameters and temperature has been studied in other literature. For instance, Płaczek et al. investigated the influence of temperature on the energy harvesting efficiency of an MFC device oscillated under tension at a fixed frequency of 1.5Hz [35]. A negative linear correlation between peak voltage and the temperature was found by their work with a change in the maximum voltage of more than 50% from -30°C to 70°C. They concluded that this change was due to the temperature dependence of the dielectric constant of the MFC. However, the authors are unaware of any study that has shown how these parameters affect the performance of energy harvesting devices and which factor dominates in the case of their integration into a co-fabricated structure.

The charge coefficient determines the capacitance parameters and therefore and indirectly affects the reactance value, Z_c, which can be expressed briefly by equations (1) and (2) [40]:

$$\mathrm{Z\_c} = \frac{1}{2\pi \mathrm{fC}} \tag{1}$$

$$\mathrm{C} = \frac{\mathrm{k}\varepsilon_{\mathrm{p}}\mathrm{A}}{\mathrm{d}} \tag{2}$$

Where f is the standard electrical frequency, ε_p is the dielectric permittivity of MFC, A is the area of the conductive plate, k is the relative permittivity and d is the distance between the conductive plates.

The capacitance at room temperature, C of the MFC used in this investigation was obtained from the product datasheet as the quoted value of 177nF (±20%) [37]. A capacitive reactance Z_c (approximately 17983Ω) was calculated from equation (1) using this value. According to the work of Płaczek et al., a linear relationship between the dielectric constant of the MFC and temperature can be assumed, resulting in a linear change of the capacitive reactance Z_c from 20631.9Ω at -35°C to 16248.6Ω at 70°C [35]. Furthermore, an MFC can be equivalently modelled as a system in which capacitance and resistance are connected in parallel and voltage is connected in series [41], so that the total reactance of the MFC can be expressed by equation (3):

$$\mathrm{Z_i} = \frac{\mathrm{Z_C Z_R}}{\mathrm{Z_C + Z_R}} \tag{3}$$

Where Z_R is the internal resistance of the MFC. According to the material composition, and approximate resistance can be assumed based on the resistivity of PZT-5 and volume of the MFC used in this experiment, which is 12.6MΩ [42]. The total reactance Z_i is equivalent to Z_c, which means the

internal resistance of MFC can be ignored. Therefore, the current generated by a piezoelectric transducer can be derived by equation (4) [29]:

$$\mathrm{I_{sc}(t)} = \omega(\mathrm{t})\mathrm{d_{31}}\sigma_{\mathrm{av}}\mathrm{A} \tag{4}$$

Where I_{SC} is the short circuit current and $\omega(t)$ is the frequency at which the piezoelectric transducer was excited. σ_{av} is the average stress acting on the piezoelectric layer and A is the active area of the piezoelectric domain. The M8528-P2 MFC device utilised in this investigation primarily harvests energy transverse to the axis of polarization, so it was assumed that the d_{31} mode was predominantly activated by the stresses produced under the peak-to-peak tension and compression caused by cantilever bending.

The parameters of A and $\omega(t)$ are invariant, while the value of the charge coefficient d_{31} is approximately linearly proportional to temperature [38,43,44]. For a load current I_{load} and an external electrical impedance Z_{load}, which is equal to 20kOhm, the electrical power of harvested energy $P(t)$ can be calculated by equations (5) and (6) [29]:

$$\mathrm{I_{load}(t)} = \frac{\mathrm{I_{sc}^2(t)Z_i}}{\sqrt{\mathrm{Z_i^2 + Z_{load}^2}}} = \frac{(\omega(\mathrm{t})\mathrm{d_{31}}\sigma_{\mathrm{av}}\mathrm{A})^2 \cdot \left(\frac{1}{2\pi \mathrm{fC}}\right)}{\sqrt{\left(\frac{1}{2\pi \mathrm{fC}}\right)^2 + \mathrm{Z_{load}^2}}} \tag{5}$$

$$\mathrm{P(t)} = \mathrm{I_{load}^2(t)Z_{load}} = \frac{\mathrm{I_{sc}^4(t)Z_{load}Z_i^2}}{\mathrm{Z_i^2 + Z_{load}^2}} \tag{6}$$

In equation (4), the temperature dependence of energy harvesting is influenced by d_{31}, σ_{av} and C. As previously shown, C increases with temperature, so that the value of the quotient $\frac{Z_i}{\sqrt{Z_i^2 + Z_{load}^2}}$ ranges from 0.718 to 0.630 based on the capacitive reactance Z_i varying between 20631.9Ω at -35°C and 16248.6Ω at 70°C. Furthermore, there is a positive correlation between d_{31} and temperature where the gradient of this relationship is dependent on the composition of the piezoelectric material. For instance, Wolf observed an increase of 29% in the magnitude of d_{31} for a PZT film with equal quantities of Zr and Ti over a temperature range from -55°C to 85°C [45]. By assuming a similar linear correlation for the M8528-P2 MFC device, it is estimated that the magnitude of d_{31} increases by 23.9% from -35°C to 70°C. It is notable that despite the positive correlation of d_{31} and small negative correlation of $\frac{Z_i}{\sqrt{Z_i^2 + Z_{load}^2}}$ with temperature, the actual output voltage of the energy harvester is negatively correlated with temperature. According to the presented calculations, the value of the parameter σ_{av} at 70°C is 0.535 times that at -40°C. This illustrates the significant effect of the parameter σ_{av}, which decreases with temperature due to the viscoelastic behaviour of the polymer matrix and therefore contributes to an overall reduction in output power $P(t)$.

In order to verify this conclusion, a relationship describing the orthotropic stresses and strains that arises from thermal expansion and contraction is obtained from classical laminate theory and is expressed in equation (7) [46]:

$$\begin{bmatrix} \sigma_1 \\ \sigma_2 \\ \tau_{12} \end{bmatrix} = \begin{bmatrix} \mathrm{Q_{11}} & \mathrm{Q_{12}} & 0 \\ \mathrm{Q_{21}} & \mathrm{Q_{22}} & 0 \\ 0 & 0 & \mathrm{Q_{66}} \end{bmatrix} \begin{bmatrix} \varepsilon_1 & -\alpha_1 \Delta \mathrm{T} \\ \varepsilon_2 & -\alpha_2 \Delta \mathrm{T} \\ \gamma_{12} & 0 \end{bmatrix} \tag{7}$$

In equation (7), σ_i are the axial stresses, Q_{ij} is the reduced stiffness matrix, τ_{12} is the in-plane shear stress, γ_{12} is the in-plane shear strain, α_i is the coefficient of thermal deformation and ΔT is the change in temperature. According to this equation, a change in temperature ΔT causes a thermal strain equal to $-\alpha_i \Delta T$, which decreases the in-plane axial stresses σ_i for a positive coefficient of thermal

expansion α_i. Thus, thermal expansion causes a decrease in the average stress σ_{av} generated on the active area of the MFC at elevated temperatures, as mentioned in equations (4), (5) and (6), which is consistent with the aforementioned inverse proportionality of σ_{av} with temperature.

From a micromechanical point of view, the viscoelastic behaviour of composites arises from greater polymer chain motion at higher temperatures, which results in a decrease in elastic modulus and a softening of the polymer matrix [47,48]. Assuming that the structure obeys a Hookean relationship of elastic deformation, the flexural stress of the cantilever will be proportionately lower for the same given strain at higher temperatures due to the corresponding decrease in stiffness. Similarly, to the effect of thermal expansion discussed for equation (7), viscoelasticity also serves to reduce the average stress parameter σ_{av} at higher temperatures, which causes an observed decrease in the output voltage of energy harvesting. A further contribution to the temperature dependence of the structure may be the relief of residual thermal stresses that arise during manufacturing. In contrast to the aforementioned effects of thermal expansion and viscoelasticity, the alleviation of thermal stresses is predicted to have a relatively minor influence on structural properties, although this is outside of the scope of this investigation.

Table 1 presents a comparison of reported findings on the influence of temperature on the energy harvesting of PZT materials or components [31,35,38,49]. These publications reported negative correlations between harvested energy and temperature, which is in agreement with the findings of this investigation. Prior research has focussed on the MFC transducer rather than multifunctional energy harvesting structures and there is variation in the methodologies employed by the researchers, including their investigation of different temperature conditions. As shown by the research opportunities identified by previous studies, the further investigation of the thermal dependence of energy harvesting in MFC devices will be pertinent to the practical application of smart composite structures.

3.3 Ambient noise vibration excitation test analysis of temperature influence

As previously shown in Fig. 5, -10 °C was found to be the optimal temperature for energy harvesting. Ambient vibration tests were conducted at temperatures between -30 °C and 30 °C at intervals that were representative of the trend observed in Fig. 5. By taking one offshore wind project from southeastern China as an example reference, tests were conducted with a humidity set-point of 70%RH to represent typical environmental conditions [50].

As previously discussed in section 3.2, the viscoelasticity of the polymer matrix influences the stiffness of the cantilever, so its resonance frequency is also affected by temperature. As shown in Fig. 6, the frequency of the first three modes of cantilever resonance decrease with temperature; the corresponding mode patterns are shown to the right side of the graph. The maximum displacement occurring in the 1st and 2nd bending modes (Mode 1, 3) and the 1st torsion mode (Mode 2) are shown by the visualisations in Fig. 6. These were obtained from FEA analysis according to the location of MFC and its operating principle through COMSOL. The finite element modelling was completely consistent with the actual experiment, including the material properties of the integration sample used, boundary conditions and so on. It can be noted that higher-order modes were associated with greater absolute changes in the magnitude of the resonance frequency as a function of temperature. The

associated changes in stiffness and resonance frequency thereby affect the energy harvested for a given amplitude of excitation.

The overall trend of the RMS voltage output with temperature for ambient vibration, shown in Fig. 7, is similar to that observed for the swept sine tests in Fig. 5, although the comparable magnitude of the energy harvested for each temperature condition was different. For the wind replicator tests shown in Fig. 7, the output voltage at 10°C is greater than the output voltage at 30°C and output at -20°C is greater than -30°C, which are inconsistent with the results previously shown for swept sine frequency experiments in Fig.5. This leads to the question, what is the reason for the difference between the results of these two experiments. One reason could be the measurement error of the experiment. As the data in Fig. 7 is the average of five measurements, their standard deviations were calculated to evaluate the dispersion, where the maximum standard deviation at -10°C is approximately 4.6% of the mean value, which is well within the acceptable margin of error. This difference between the results of two experiments can be due to the vibration profiles applied by the swept sine and wind replicator tests. In the former, the amplitude of input vibration was constant, whereas for the latter the amplitude varied in the frequency domain. Exploring the magnitude and reasons of the differences can verify the correlation between the results of swept frequency vibration experiment and ambient vibration experiment.

The harvested energy is maximal when the amplitude of bending of the cantilever is greatest, which occurs when the frequency of excitation coincides with the frequency of the first mode of resonance of the cantilever. This occurs between 21.23Hz and 22.366Hz for the range of temperatures shown in Fig. 6. Obviously, the frequency changing with temperatures for mode 1 is negligible. Meanwhile, as shown in Fig. 4, the output voltage of the MFC is substantially lower at frequencies below 100Hz for all temperatures and this serves to reduce the contribution of the first mode of resonance to the overall magnitude of harvested energy. In contrast, the second and third modes of resonance occur at frequencies above 100Hz for which the output voltage of the MFC device is greater, so their contributions to harvested energy are proportionately higher than might be suggested by the shape of their deflections. Figure 8 presented the input frequency domain signal of ambient vibration(blue) and swept vibration(purple) excitation. From the point of view of the input signal, the excitation amplitude of swept frequency signal is stable, while the ambient vibration profile is not smooth and is characterised by sharp peaks, as shown in Fig. 8. However, according to the nature of the resonance phenomenon, resonance occurs when the excitation frequency is close to the resonant frequency of the stimulated sample, where these resonant frequencies would change with temperature, as the yellow and red vertical line shown in Fig.8. No matter how large the peaks at other frequencies are, they have little effect on the energy output, and only the excitation amplitudes at resonance frequencies are more valuable. Therefore, it can be noted that there is a significant difference in the frequencies at which the second and third modes of resonance occur for temperatures of 10°C and 30°C. As shown by the highlighted insets, this difference in frequency of the second and third resonance modes causes them to coincide with different amplitude peaks of the ambient vibration profile. Therefore, in addition to the general trend of greater energy harvesting at lower temperatures that was described in section 3.2, the magnitude of harvested energy from ambient vibration is also influenced by the temperature dependence of resonance excitation shown in Fig.6 and the nonlinear frequency dependence of voltage output shown in Fig. 4. Meanwhile, the overall trend of swept frequency vibration experiment and ambient vibration experiment results are basically the same. Thus, the swept frequency test result can predict the ambient test.

While the efficacy of energy harvesting of the MFC device has been shown to be dependent on temperature, the strong influence of resonance on the magnitude of VRMS in Fig. 6 highlights the

importance of structural properties of the application in determining the performance of MFC energy harvesting devices. This includes the geometry and stiffness of the structure, the means by which it is constrained and excited and the profile of the random vibration that the application will experience during service.

The humidity effect on energy harvesting

As described in [51], The average temperature in England throughout the year is approximately 10°C, with maximum temperatures exceeding 30°C in summer. The influence of humidity on energy harvesting was studied at these two reference temperatures to represent a typical range of hygrothermal conditions in the UK. Similarly, FFT analysis of the first three modes resonance frequency for the cantilever was presented in Fig. 9. It demonstrates that there was a negligible variation in the frequency at which these resonance peaks occurred for tests at the same temperature of 30°C with variation in humidity at 10%RH, 30%RH, 50%RH, 70%RH, 90%RH, which suggests that humidity did not significantly affect the resonant properties of the cantilever.

It should be noted that this study of the influence of humidity was undertaken with the methodology described in section 2.2 so that tests were started immediately once the temperature and humidity within the climatic chamber had reached equilibrium. This timescale is insufficient for obtaining moisture equilibrium within composite samples due to the slow process of diffusion of water into the polymer matrix [52]. These results, therefore, do not reflect the long-term influence of moisture uptake on the composite sample. Since Young's modulus of glass fibre reinforced epoxy is known to decrease due to swelling of the matrix with water [53], it can be expected that longer exposure in more humid environments will decrease the harvested energy. Previous analysis classified that the EH change at 10°C and 30°C is caused by input vibration. Nevertheless, the swept and ambient test were processed at different humidity condition. Therefore, a comparison of the humidity sensitivity of measured voltage outputs in experiments at temperatures of 10°C and 30°C is illustrated to explain how much humidity matters in these two experiments, as shown in Fig. 10.

It is showing a clear change of the output voltage measured at different humidity levels in Fig. 10, however, it is worth to notice that it is less significant because the change was shown due to an enlarged scale of the vertical axis as a focus. With a calculation of the standard deviation of the voltage output generated at the humility of 10%RH, 30%RH, 50%RH, 70%RH, 90%RH, respectively, the errors are found to be 3.36% for 10°C and 2.87% for 30°C separately, both of errors are far under 5%. The humidity sensitivity is hence to be negligible than the findings tested for temperatures' study in Fig. 7.. Furthermore, according to the aforementioned conclusion by Fig.9, short-term exposure to humidity seemed to have a minor effect on the mechanical resonance properties of the cantilever, although it may be attributed to electrical parameters of the MFC transducer on humidity variation. This was proven by the work of Lipscomb et al., where the resistance of a single piezo-ceramic was indeed associated with humidity factors [54]. But our work is integrating the energy harvesters with composite structure together as a full functional device, that might be the reason to show a slight effect by humidity factor based on our experimental measurements. In our future study, r the focus to disambiguate the effects of humidity on the mechanical and electrical properties of such integrated composite structures, will be investigated.

Conclusion

A glass fibre composite cantilever sample was subjected to swept sine frequency and wind field ambient vibration profiles in order to investigate the effect of temperature and humidity on the energy harvesting of integrated functional composite.

The swept sine tests showed strong correlations between the output voltage and temperature, with a general trend of greater energy harvesting at lower temperatures. In addition, swept sine testing also showed that the voltage amplitudes varied with frequency and tended to increase in magnitude from low frequencies towards a plateau at 100Hz. In addition, this investigation has considered the influence of electrical parameters, including the dielectric constant and charge coefficient on energy harvesting. Theoretical analysis confirms a negative correlation between the temperature and the flexural stiffness and strength of the structure, which is also the dominant factor affecting the power output of energy harvesting.

Testing with a wind field ambient vibration profile demonstrated the suitability of the integrated energy harvesting device for the practical application of vibration harvesting from a wind turbine. The result analysis showed how the temperature dependence of the frequencies of flexural and torsional modes of resonance affected the magnitude of harvested energy, which resulted in minor differences from the outcome of the swept sine experiments. The output of energy harvesting was more strongly correlated with temperature than humidity. Resonance frequencies were not measurably affected by humidity for the short periods of hygrothermal conditioning permitted by the methodology, so the observed nonlinear influence of humidity on energy harvesting may have arisen from the effect of humidity on the electrical properties of the sensor. Further work should investigate temperature by including longer periods of climatic conditioning to investigate the long-term effect of moisture update on the efficacy of energy harvesting.

In conclusion, the research has shown the feasibility of an energy harvester device integrated with MFC transducer under extreme environmental conditions, where the efficiency of the power output varied with the temperature and humidity. Temperature affected both the mechanical and electrical properties of the integrated energy harvesting device, while energy harvesting was dominated by the structural properties of the composite cantilever. This study promotes the practice of smart multifunctional composite materials and provides a parametric consideration for the potential influence factors in practical application from multiple perspectives.

Acknowledgement

This research was supported by Innovate UK (Project Reference 104030). Original vibration data collection and measurement was undertaken and supported by industrial collaboration partner Titan Wind Ltd. Vibration testing was undertaken by WMG with the kind encouragement of Prof. James Marco and David Williams and the support of the High Value Manufacturing Catapult.

References

1. Gibson, R.F., *A review of recent research on mechanics of multifunctional composite materials and structures.* Composite Structures, 2010. **92**(12): p. 2793-2810.

2. Narayana, K.J. and R. Gupta Burela, *A review of recent research on multifunctional composite materials and structures with their applications.* Materials Today: Proceedings, 2018. **5**(2, Part 1): p. 5580-5590.

3. Chung, D.D.L., *A review of multifunctional polymer-matrix structural composites.* Composites Part B: Engineering, 2019. **160**: p. 644-660.

4. Tuna, G. and V.C. Gungor, *2 - Energy harvesting and battery technologies for powering wireless sensor networks*, in *Industrial Wireless Sensor Networks*, R. Budampati and S. Kolavennu, Editors. 2016, Woodhead Publishing. p. 25-38.

5. Wilson, W.C. and P.D. Juarez, *Emerging Needs for Pervasive Passive Wireless Sensor Networks on Aerospace Vehicles.* Procedia Computer Science, 2014. **37**: p. 101-108.

6. Leccese, F., et al. *Analysis, design, realization and test of a sensor network for aerospace applications*. in *2017 IEEE International Instrumentation and Measurement Technology Conference (I2MTC)*. 2017.

7. Jia, Y., et al., *A Numerical Feasibility Study of Kinetic Energy Harvesting from Lower Limb Prosthetics.* Energies, 2019. **12**(20).

8. Xu, T.B., *7 - Energy harvesting using piezoelectric materials in aerospace structures*, in *Structural Health Monitoring (SHM) in Aerospace Structures*, F.-G. Yuan, Editor. 2016, Woodhead Publishing. p. 175-212.

9. Abdelkareem, M.A.A., et al., *Vibration energy harvesting in automotive suspension system: A detailed review.* Applied Energy, 2018. **229**: p. 672-699.

10. Ghomian, T. and S. Mehraeen, *Survey of energy scavenging for wearable and implantable devices.* Energy, 2019. **178**: p. 33-49.

11. Hamid, R. and M.R. Yuce, *A wearable energy harvester unit using piezoelectric–electromagnetic hybrid technique.* Sensors and Actuators A: Physical, 2017. **257**: p. 198-207.

12. Wymore, M.L., et al., *A survey of health monitoring systems for wind turbines.* Renewable and Sustainable Energy Reviews, 2015. **52**: p. 976-990.

13. Wang, P., et al., *Investigation of Wireless Sensor Networks for Structural Health Monitoring.* Journal of Sensors, 2012. **2012**: p. 7.

14. Yang, B. and D. Sun, *Testing, inspecting and monitoring technologies for wind turbine blades: A survey.* Renewable and Sustainable Energy Reviews, 2013. **22**: p. 515-526.

15. Lian, J., et al., *Health Monitoring and Safety Evaluation of the Offshore Wind Turbine Structure: A Review and Discussion of Future Development.* Sustainability, 2019. **11**(2).

16. Niezrecki, C., et al., *Inspection and monitoring of wind turbine blade-embedded wave defects during fatigue testing.* Structural Health Monitoring, 2014. **13**(6): p. 629-643.

17. Lestari, I. and M. Arafat, *A review of wireless sensor networks for structural health monitoring: offshore wind turbines deployment.* Journal of Physics: Conference Series, 2019. **1150**: p. 012005.

18. Hamdan, A., M.T.H. Sultan, and F. Mustapha, *11 - Structural health monitoring of biocomposites, fibre-reinforced composites, and hybrid composite*, in *Structural Health*

Monitoring of Biocomposites, Fibre-Reinforced Composites and Hybrid Composites, M. Jawaid, M. Thariq, and N. Saba, Editors. 2019, Woodhead Publishing. p. 227-242.

19. Sebastian, R.K., S. Perinpinayagam, and R. Choudhary, *Health Management Design Considerations for an All Electric Aircraft.* Procedia CIRP, 2017. **59**: p. 102-110.

20. Giglio, M., A. Manes, and C. Sbarufatti, *9 - MEMS for structural health monitoring in aircraft*, in *MEMS for Automotive and Aerospace Applications*, M. Kraft and N.M. White, Editors. 2013, Woodhead Publishing. p. 220-244.

21. Yang, Z., et al., *High-Performance Piezoelectric Energy Harvesters and Their Applications.* Joule, 2018. **2**(4): p. 642-697.

22. Shirvanimoghaddam, M., et al., *Towards a Green and Self-Powered Internet of Things Using Piezoelectric Energy Harvesting.* IEEE Access, 2019. **7**: p. 94533-94556.

23. Elahi, H., M. Eugeni, and P. Gaudenzi, *A Review on Mechanisms for Piezoelectric-Based Energy Harvesters.* Energies, 2018. **11**(7).

24. Sodano, H.A., *Macro-fiber composites for sensing, actuation and power generation*. 2003, Virginia Tech.

25. Todaro, M.T., et al., *Piezoelectric MEMS vibrational energy harvesters: Advances and outlook.* Microelectronic Engineering, 2017. **183-184**: p. 23-36.

26. Friswell, M.I., et al., *Non-linear piezoelectric vibration energy harvesting from a vertical cantilever beam with tip mass.* Journal of Intelligent Material Systems and Structures, 2012. **23**(13): p. 1505-1521.

27. Caliò, R., et al., *Piezoelectric Energy Harvesting Solutions.* Sensors, 2014. **14**(3).

28. Shi, Y., S.R. Hallett, and M. Zhu, *Energy harvesting behaviour for aircraft composites structures using macro-fibre composite: Part I – Integration and experiment.* Composite Structures, 2017. **160**: p. 1279-1286.

29. Jia, Y., et al., *Multiphysics vibration FE model of piezoelectric macro fibre composite on carbon fibre composite structures.* Composites Part B: Engineering, 2019. **161**: p. 376-385.

30. Alsaadi, A., et al., *Vibration energy harvesting of multifunctional carbon fibre composite laminate structures.* Composites Science and Technology, 2019. **178**: p. 1-10.

31. Arroyo, E., et al., *Experimental and Theoretical Study of a Piezoelectric Vibration Energy Harvester Under High Temperature.* Journal of Microelectromechanical Systems, 2017. **26**(6): p. 1216-1225.

32. Bai, Y., T. Keller, and T. Vallée, *Modeling of stiffness of FRP composites under elevated and high temperatures.* Composites Science and Technology, 2008. **68**(15): p. 3099-3106.

33. Manalo, A., et al., *Temperature-sensitive mechanical properties of GFRP composites in longitudinal and transverse directions: A comparative study.* Composite Structures, 2017. **173**: p. 255-267.

34. X. Li, L. Wu, L. Ma, and X. Yan, “Effect of temperature on the compressive behavior of carbon fiber composite pyramidal truss cores sandwich panels with reinforced frames,” Theor. Appl. Mech. Lett., vol. 6, no. 2, pp. 76–80, 2016.

35. M. Płaczek and G. Kokot, “Modelling and laboratory tests of the temperature influence on the efficiency of the energy harvesting system based on MFC piezoelectric transducers,” Sensors (Switzerland), vol. 19, no. 7, 2019.

36. M. S. Yoon, I. Mahmud, and S. C. Ur, “Phase-formation, microstructure, and piezoelectric/dielectric properties of BiYO3-doped Pb(Zr0.53Ti0.47)O3 for piezoelectric energy harvesting devices,” Ceram. Int., vol. 39, no. 8, pp. 8581–8588, 2013.

37. Smart Material. Mfc product properties [cited 10 February 2020 2018] URL www. smart-material.com/MFC-product-properties.html.

38. X. Lin et al., “Investigation of temperature sensitivity of actuation performance for piezoelectric fiber composites,” Ceram. Int., vol. 43, no. 13, pp. 10590–10594, 2017.

39. Cotes (2015) ‘Wind Turbines Need Protecting Against the Effects of Humidity’, pp. 5–9. Available at: https://einpart.com/files/catalogs/WTG_components/Cotes-On-Shore.pdf.

40. B. John, *Electrical Circuit Theory and Technology*. Elsevier, 2010.

41. S. Du, Y. Jia, C. D. Do, and A. A. Seshia, “An Efficient SSHI Interface with Increased Input Range for Piezoelectric Energy Harvesting under Variable Conditions,” *IEEE J. Solid-State Circuits*, vol. 51, no. 11, pp. 2729–2742, 2016.

42. W. Hooker, “Properties Ceramics of PZT-Based Piezoelectric and 250 ° C,” no. September, 1998.

43. C. K. Wong, Y. M. Poon, and F. G. Shin, “Temperature dependence of the complex effective piezoelectric coefficient of ferroelectric 0-3 composites,” J. Appl. Phys., vol. 92, no. 6, pp. 3287–3292, 2002.

44. N. A. Shepelin et al., “New developments in composites, copolymer technologies and processing techniques for flexible fluoropolymer piezoelectric generators for efficient energy harvesting,” Energy Environ. Sci., vol. 12, no. 4, pp. 1143–1176, 2019.

45. R. A. Wolf and S. Trolier-McKinstry, “Temperature dependence of the piezoelectric response in lead zirconate titanate films,” *J. Appl. Phys.*, vol. 95, no. 3, pp. 1397–1406, 2004.

46. R. M. Jones, *Mechanics Of Composite Materials*, 2nd Edition. Boca Raton, 1999.

47. S. Kumarasamy, M. S. Zainol Abidin, M. N. Abu Bakar, M. S. Nazida, Z. Mustafa, and A. Anjang, “Effects of High and Low Temperature on the Tensile Strength of Glass Fiber Reinforced Polymer Composites,” IOP Conf. Ser. Mater. Sci. Eng., vol. 370, no. 1, 2018.

48. R. F. Gibson, “A review of recent research on mechanics of multifunctional composite materials and structures,” Compos. Struct., vol. 92, no. 12, pp. 2793–2810, 2010.

49. S. B. Kim, J. H. Park, H. Ahn, D. Liu, and D. J. Kim, “Temperature effects on output power of piezoelectric vibration energy harvesters,” *Microelectronics J.*, vol. 42, no. 8, pp. 988–991, 2011.

50. Yue, W., Xue, Y. and Liu, Y. (2017) ‘High Humidity Aerodynamic Effects Study on Offshore Wind Turbine Airfoil/Blade Performance through CFD Analysis’, *International Journal of Rotating Machinery*, 2017. doi: 10.1155/2017/7570519.

51. Kendon, M. *et al.* (2019) 'State of the UK climate 2018', *International Journal of Climatology*, 39(S1), pp. 1–55. doi: 10.1002/joc.6213.

52. Dowdeswell, R. (2004) *Electrical impedance*, *Detecting Foreign Bodies in Food*. doi: 10.1016/B978-1-85573-729-7.50016-0.

53. Donnini, J. (2019) 'Durability of glass FRCM systems: Effects of different environments on mechanical properties', *Composites Part B: Engineering*. Elsevier Ltd, 174(April), p. 107047. doi: 10.1016/j.compositesb.2019.107047.

54. I. P. Lipscomb, P. M. Weaver, J. Swingler, and J. W. McBride, "The effect of relative humidity, temperature and electrical field on leakage currents in piezo-ceramic actuators under dc bias," *Sensors Actuators, A Phys.*, vol. 151, no. 2, pp. 179–186, 2009.

Figure:

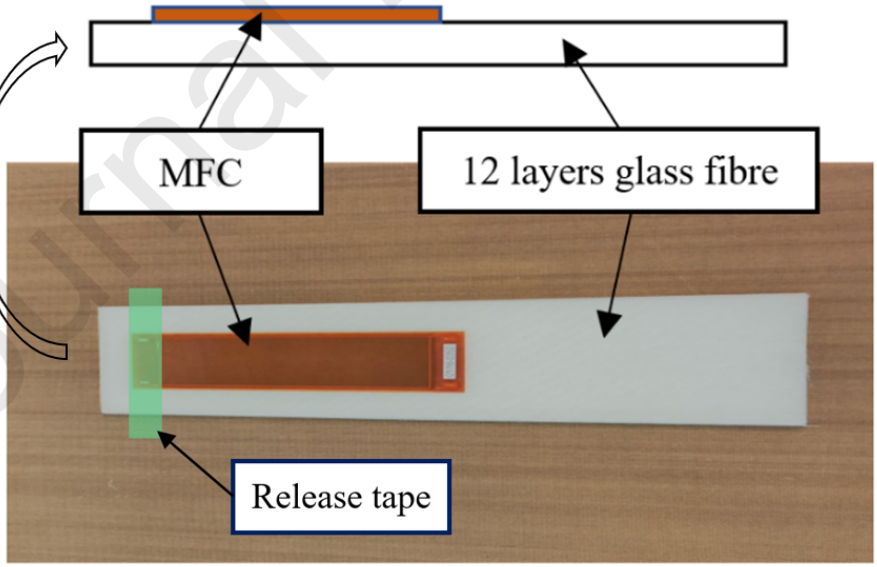

Figure 1 Schematic diagram of the co-manufacturing of the glass fibre laminate sample with MFC device.

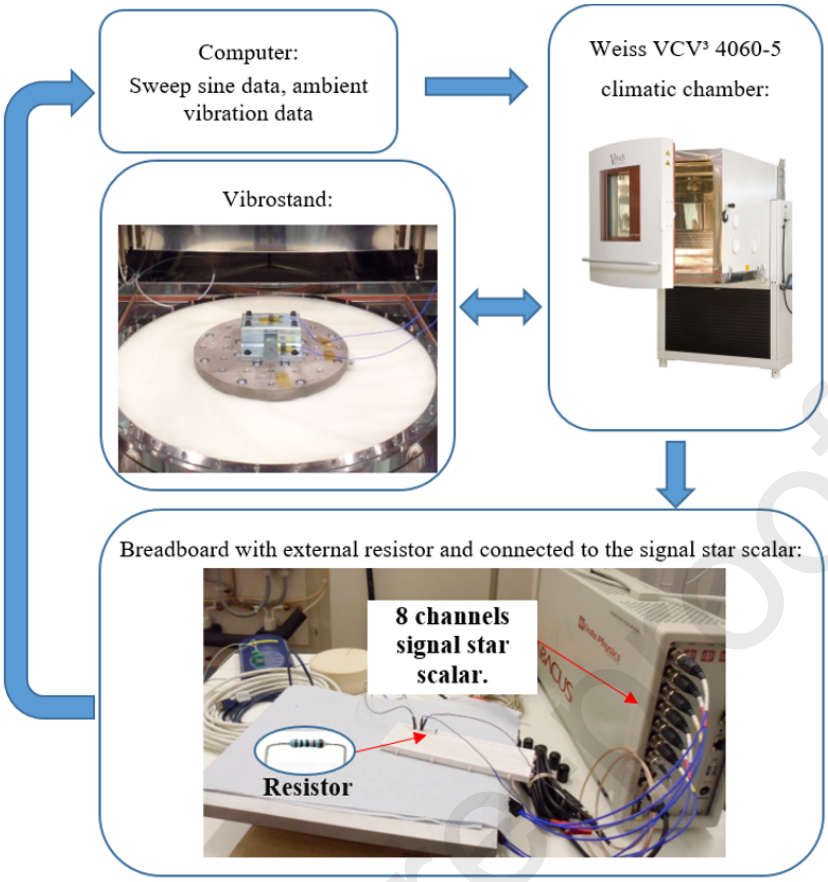

Figure 2 Experimental setup for vibration testing of the integrated MFC-on-GFRP sample. A pre-defined excitation profile (swept sine or replicator vibration data) generated by the computer was amplified and transmitted to the shaker. The shaker is fixed in the climatic chamber. The voltage output through the external resistor (20kΩ) is recorded by the SignalStar Scalar control system, then feedback to the computer.

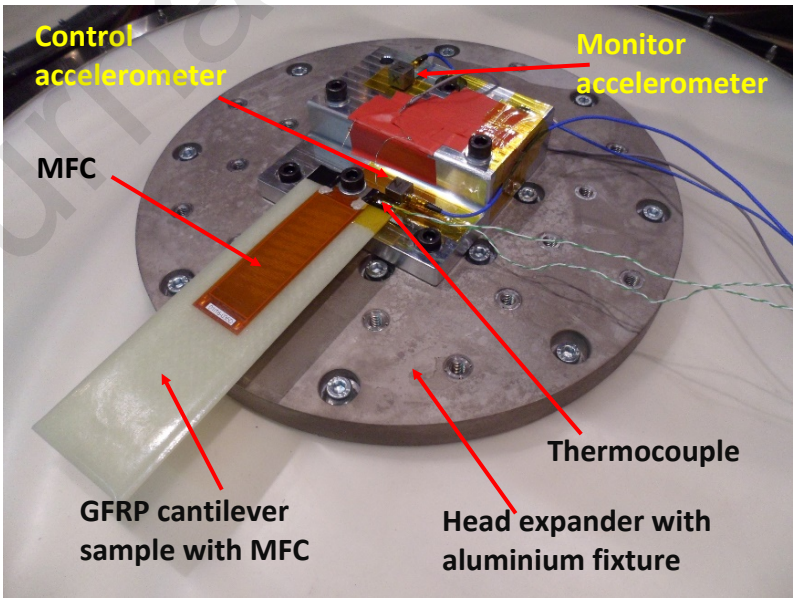

Figure 3 Cantilever sample and instrumentation for vibration testing in climatic chamber. K-type thermocouples were utilised for temperature measurement. Two accelerometers were applied for

the control and monitoring purpose to ensure the consistency of the excitation condition near to the centre of the fixture with the excitation condition near to the sample.

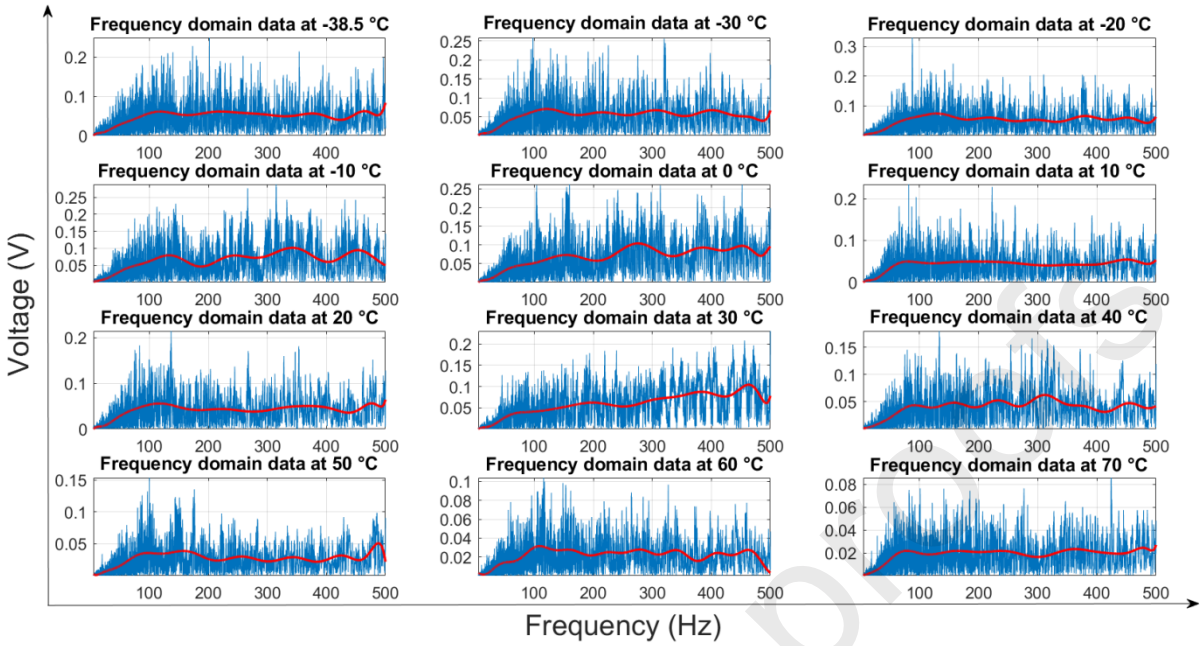

Figure 4 The RMS voltage output of Swept test in the frequency domain at different temperatures with fitted trend lines shown in red. The humidity is set up at 50%RH, temperature ranges from -38.5°C to 70°C

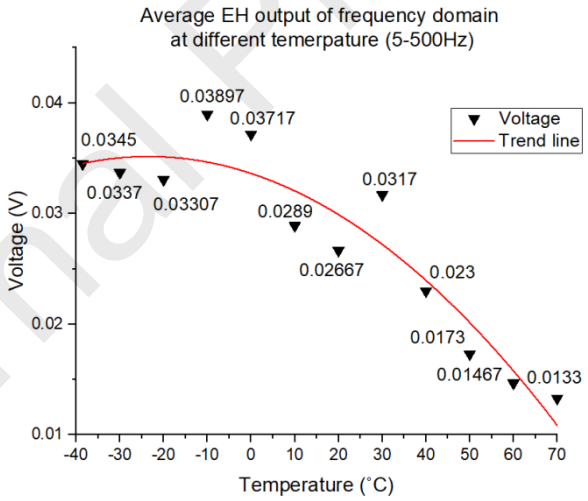

Figure 5 The averaged mean VRMS of Swept test in the frequency domain and trend line for a range of temperatures.

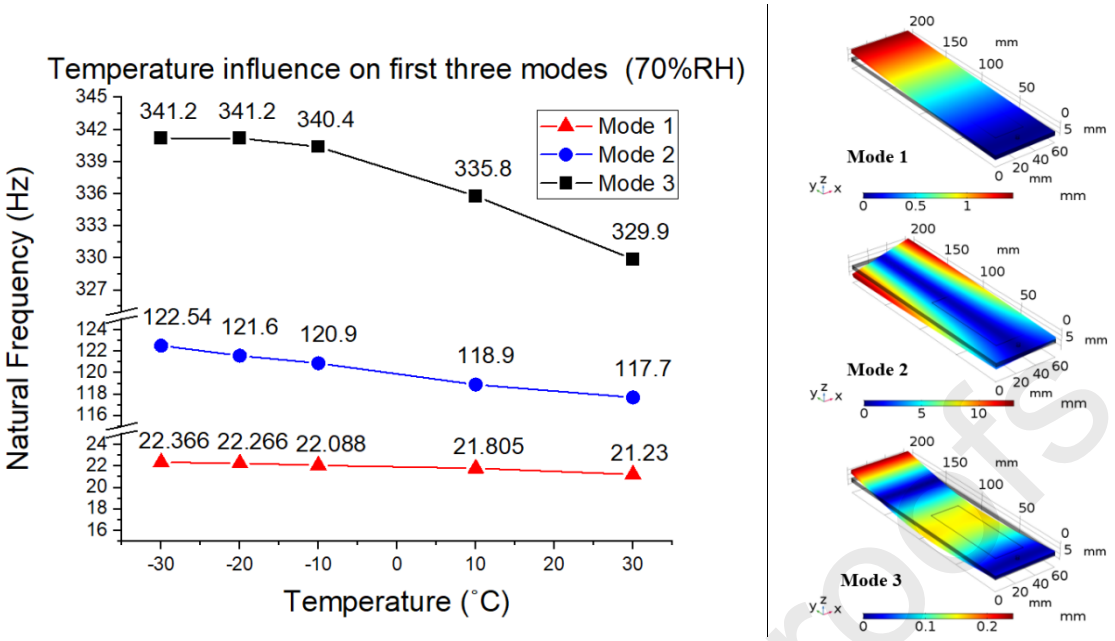

Figure 6 Temperature dependence at 70%RH of the ambient vibration test within the first three modes resonance frequency of the cantilever, which include the Mode 1(1st bending), Mode 2(1st torsion) and Mode 3(2nd bending).

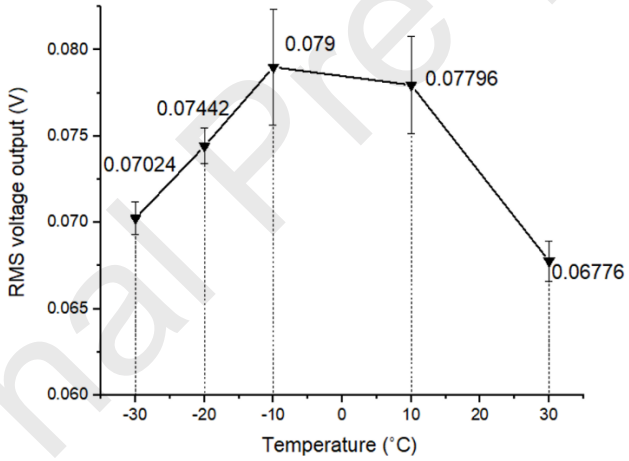

Figure 7 Temperature dependence of mean VRMS of harvested electrical energy within ambient vibration test. Datapoints represent the average of five measurements and the error bars represent one standard deviation for these mean data.

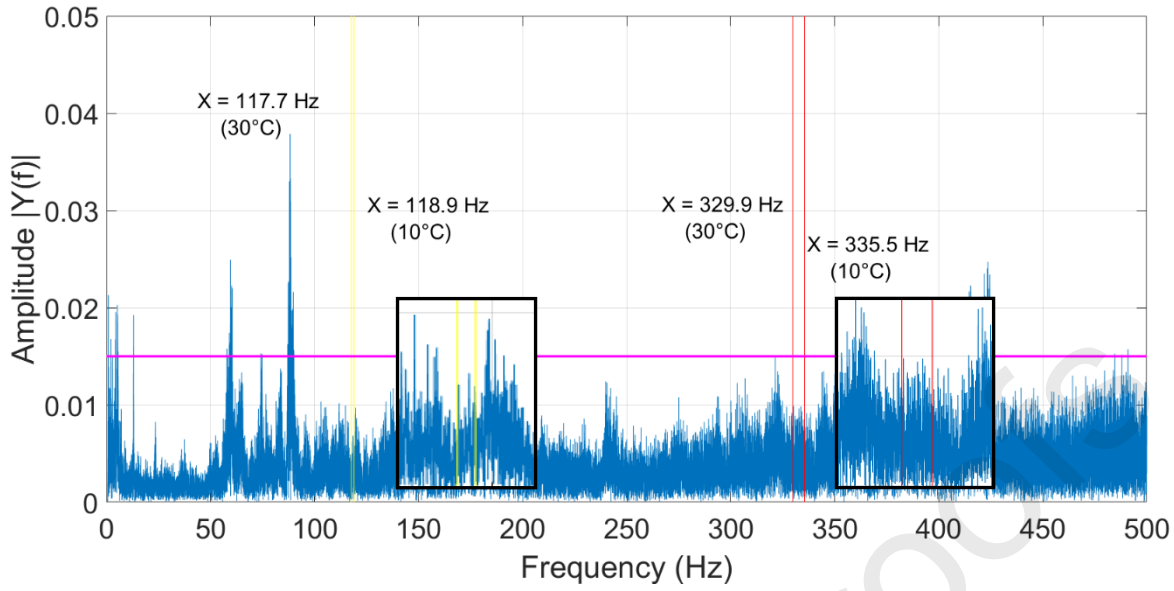

Figure 8 The FFT of ambient vibration excitation input data to the frequency domain. The purple line is the input swept frequency excitation in frequency domain. The yellow and red lines are the respective frequencies of the 2nd and 3rd modes of resonance of the sample at 10 and 30 °C. Subfigures are the enlarged view around the target frequency.

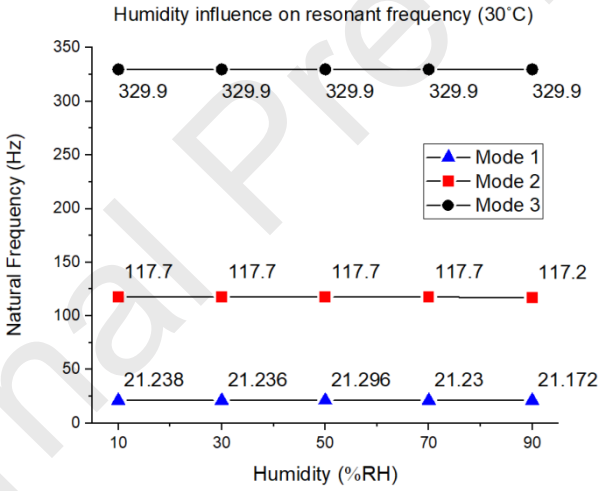

Figure 9 Variation of the frequency of the 1st, 2nd and 3rd modes of resonance with humidity at 30°C.

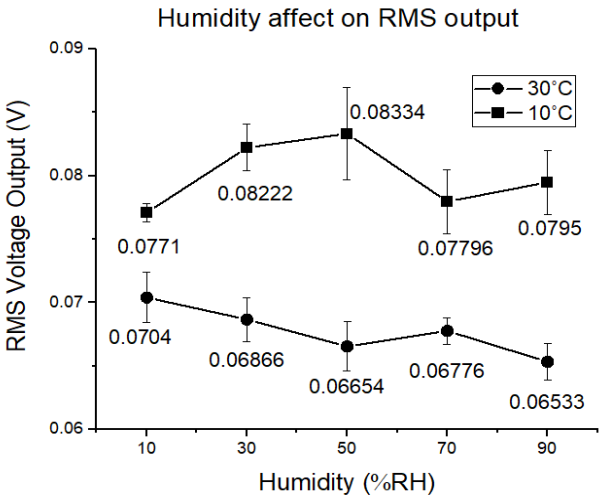

Figure 10 Comparison of effect of humidity on VRMS at 10°C and 30°C. The data is the average of five measurements and error bar represents one standard deviation from the mean for these data.

Table:

Authors/year	Material	Power/voltage vs temperature	Temperature range	Factors influencing the efficacy of energy harvesting
Kim, S./2011 [49]	Soft and hard PZT	Negative correlation	25 – 150 °C	Mainly the eletrical properties
Lin, X./2017 [38]	PZT-51 fiber	Negative correlation	-15 – 80 °C	Mainly the eletrical properties
Arroyo, E./2017 [31]	PZT	Negative correlation	20 – 160 °C	50% Mechanical quality factor and 30% thermal stresses
Płaczek, M./2019 [35]	PZT-5 (MFC-8528-P2)	Negative correlation	-30 – 70 °C	Mainly the eletrical properties

Table 1. Comparison of reported findings of the influence of temperature on energy harvesting.